

D.S.P. based Field Oriented Control of Induction motor

Adhithya S 200901002
Anabhayan S P 200901008

Under the guidance of Dr S Rama Reddy
Dean - Electrical sciences

*Department of Electrical and Electronics Engineering
Rajalakshmi Engineering college*

Field Oriented Control

- ▶ Add awesome images for indicating concept of FOC.

Introduction to Vector Control of Induction Motor

- ▶ Decouples stator current components in a rotating reference frame
- ▶ Offers better dynamic response, speed accuracy, efficiency, and power factor
- ▶ Requires complex math ops: coordinate transformations, vector calculations, and PWM generation
- ▶ Rotor flux angle estimation via sensorless techniques or physical sensors

Advantages of Field Oriented Control (FOC)

- ▶ **Dynamic Response:** Faster and more accurate response to changes.
- ▶ **Efficiency:** Reduced energy consumption and increased performance.
- ▶ **Speed Control:** Precise and accurate control of motor's speed.
- ▶ **Starting Torque:** High initial force for heavy-duty applications.
- ▶ **Regenerative Capability:** Energy recovery through regenerative braking.

Block Diagram of Field Oriented Control

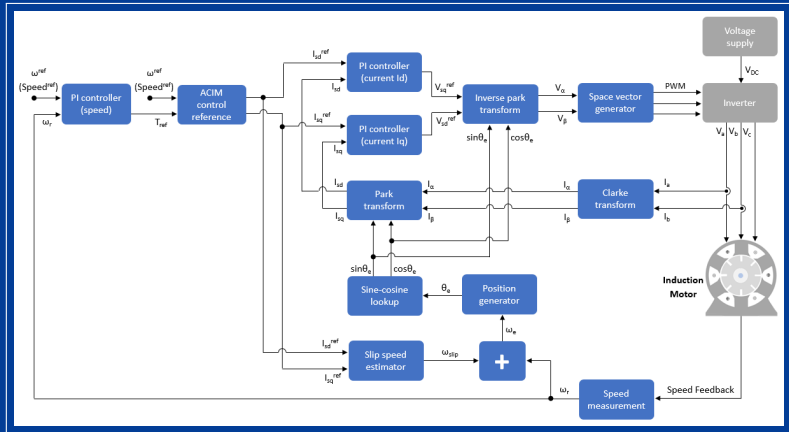
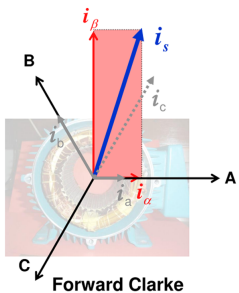


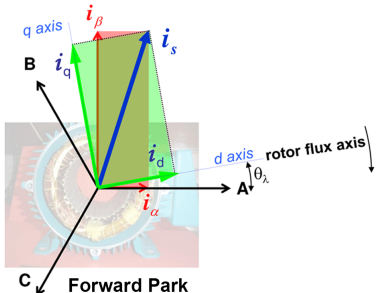
Figure: Block Diagram of Field Oriented Control

- ▶ Coordinate Transformations.
- ▶ PI Controllers.
- ▶ PWM Generation.

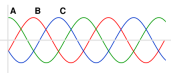
Coordinate Transformations



Forward Clarke

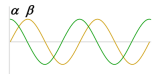


Forward Park



Forward Clarke

$$\begin{aligned}\alpha &= A \\ \beta &= \frac{(B - C)}{\sqrt{3}}\end{aligned}$$



Forward Park

$$\begin{aligned}i_d &= i_\alpha \cos \theta_\lambda + i_\beta \sin \theta_\lambda \\ i_q &= -i_\alpha \sin \theta_\lambda + i_\beta \cos \theta_\lambda\end{aligned}$$



Figure: Coordinate Transformations

Block Diagram of the System

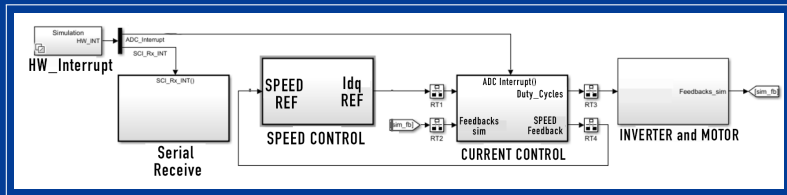


Figure: Block Diagram of the System

Speed Control Subsystem

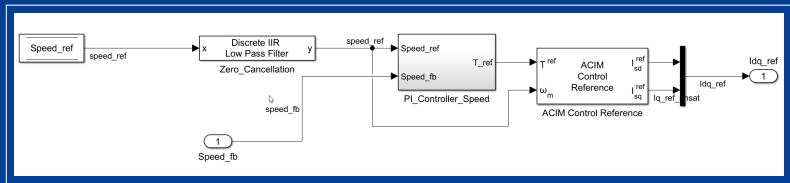
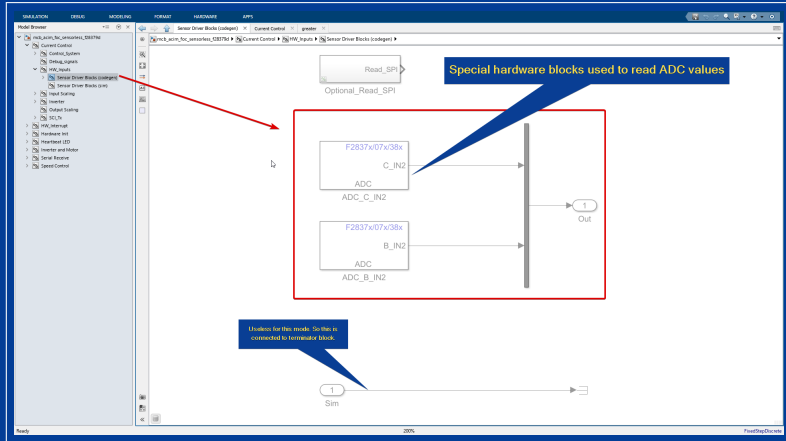
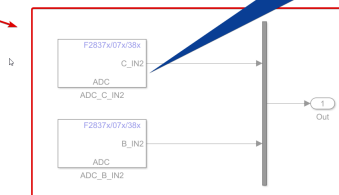


Figure: Speed Control Subsystem

Current Measurement



Special hardware blocks used to read ADC values



Useless for this mode. So then is connected to terminator block.



Figure: ADC block for reading current

Position and Speed Estimation

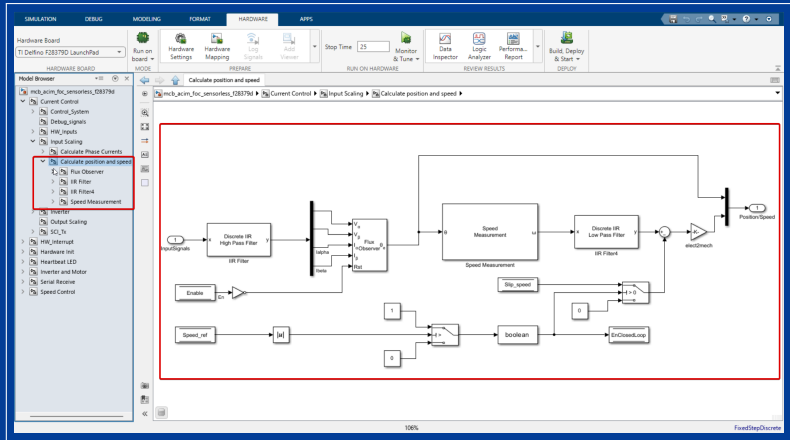


Figure: Position and Speed Estimation

Current Control System

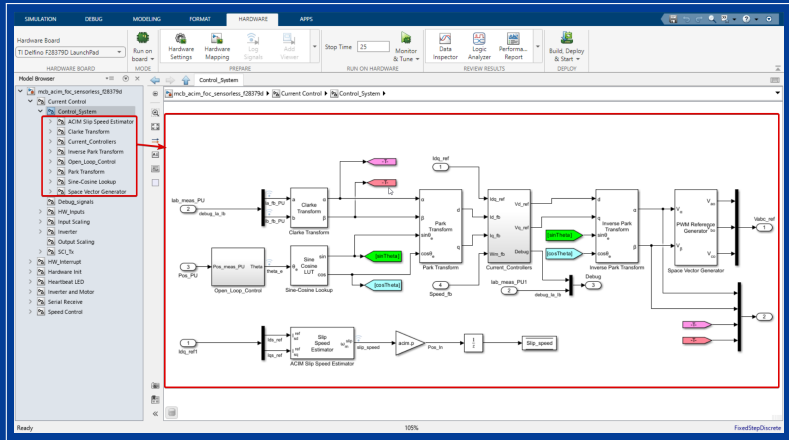


Figure: Current Control System

Speed Response

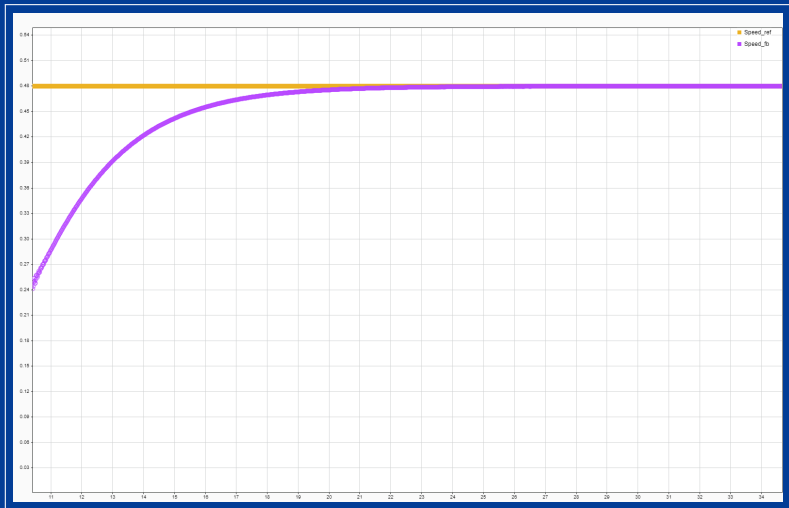


Figure: Speed Response

Slip Speed

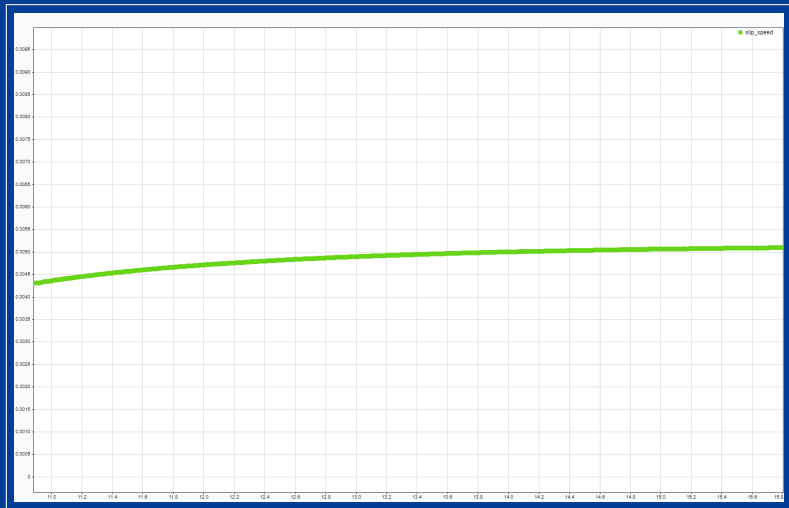


Figure: Slip Speed

Ia and Ib Feedback/Measured Currents

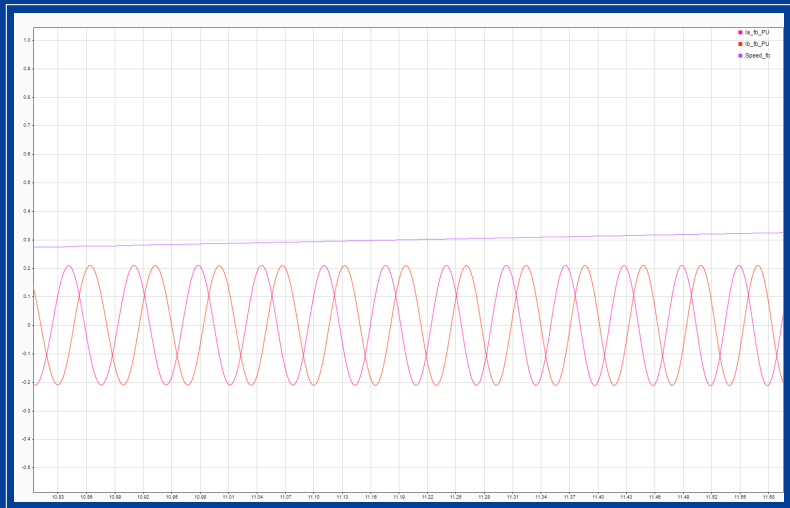


Figure: Ia and Ib Feedback/Measured Currents

Id and Iq Reference Currents

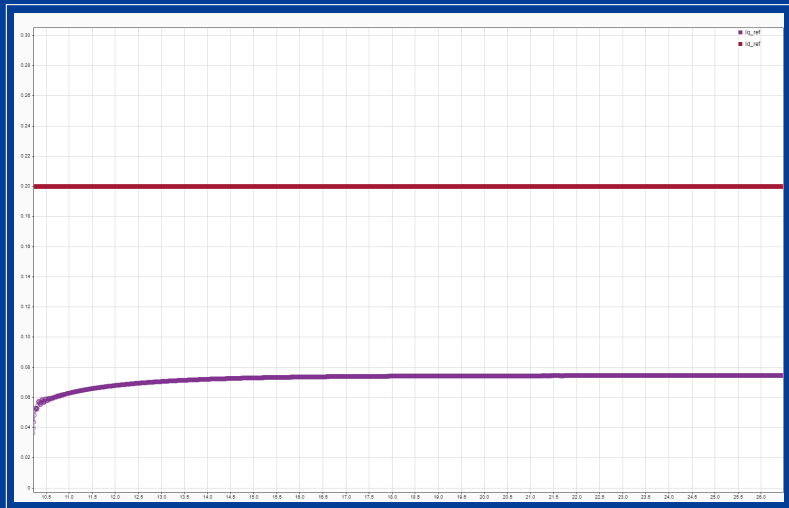
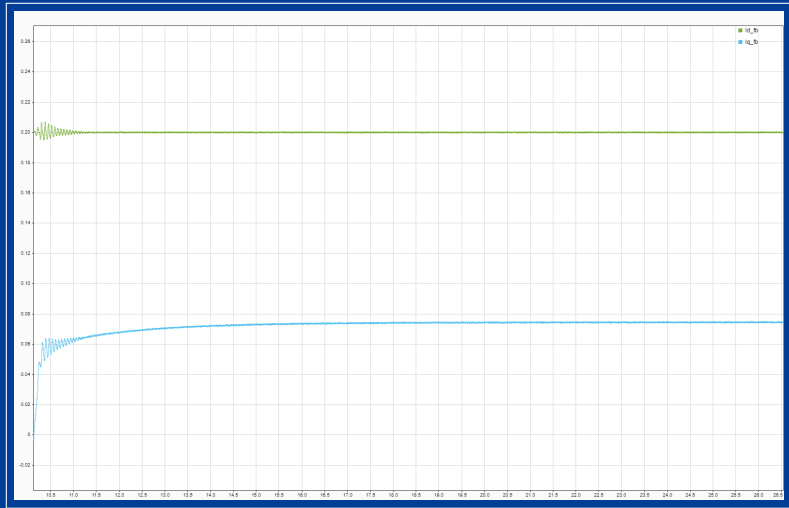
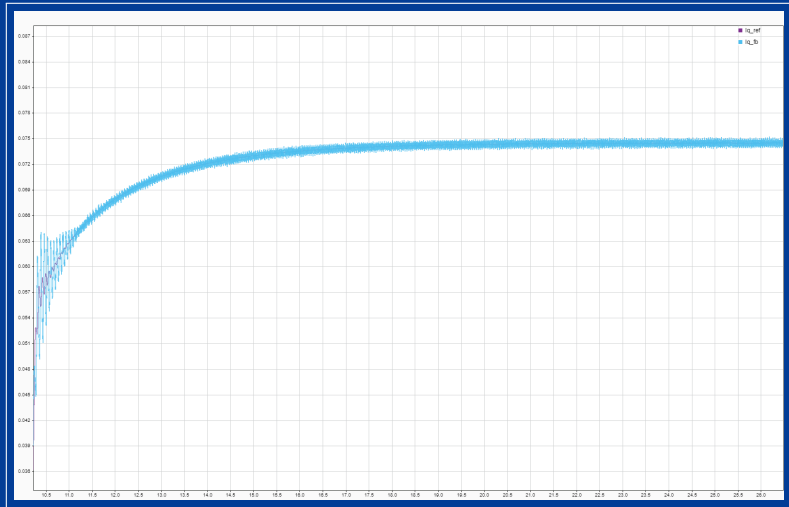


Figure: Id and Iq Reference Currents

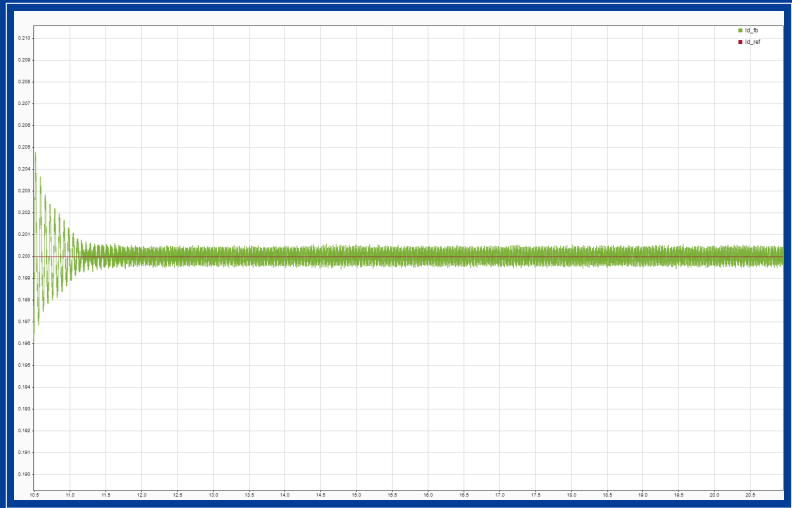
Id and Iq Feedback Currents



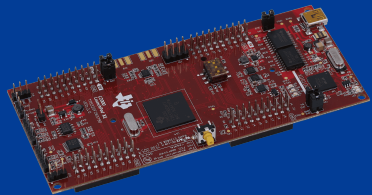
Iq Reference and Feedback Currents (Torque producing current)



Id Reference and Feedback Currents (Magnetizing current)



C2000 Features for Implementing Vector Control Algorithm



- ▶ 200 MHz C28x CPU
- ▶ Control Law Accelerator (CLA)
- ▶ 12-bit/16-bit ADCs
- ▶ Enhanced Pulse Width Modulators (ePWM)

Intelligent Power Module FSAM20SH60A

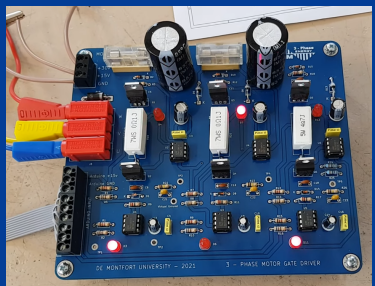


Figure 1. Package Overview

Figure: Intelligent Power Module FSAM20SH60A

- ▶ **Compact Design:** Integrates power devices, drivers, and protection circuitry.
- ▶ **Enhanced Performance:** Optimized for high-speed switching.
- ▶ **Protection Features:** Includes built-in under-voltage lockout, over-temperature protection, and fault reporting, enhancing system reliability.
- ▶ **Ease of Use** Simplifies system design and reduces time-to-market compared to designing with discrete components.

Discrete inverter vs IPM



(a) Discrete Inverter



Figure 1. Package Overview

(b) Intelligent Power Module (IPM)

Figure: Discrete Inverter vs Intelligent Power Module (IPM)

Induction Motor



Figure: Induction Motor

| Parameter | Value |
|-----------|-----------------|
| Power | 0.25 Hp |
| Voltage | 415 V (L-L) RMS |
| Current | 1.4 A |
| Frequency | 50 Hz |
| Speed | 1440 rpm |
| Phase | 3 |

Table: Name-plate Details of Induction motor

Hardware block diagram

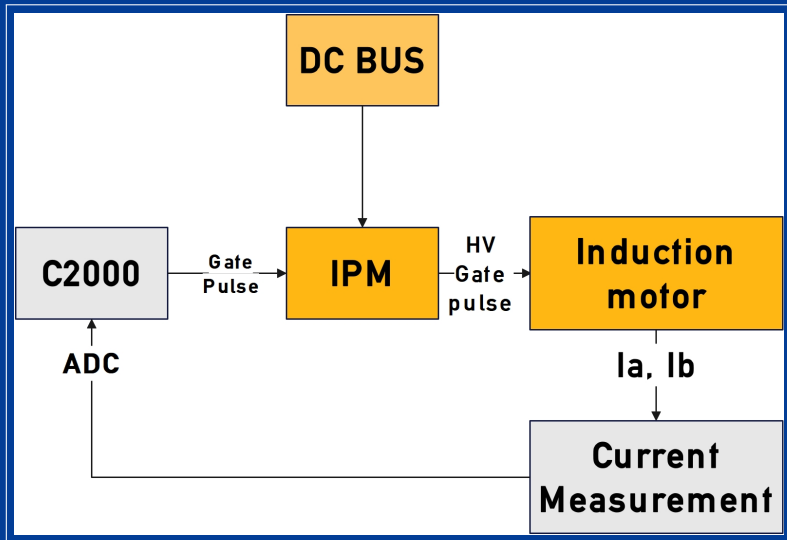


Figure: Hardware block diagram

ACIM Parameter Estimation: No-Load Test



Figure: No-load test setup



Figure: Fluke 434 power analyzer

- ▶ Slip speed is made zero.

ACIM Parameter Estimation: Test Circuits

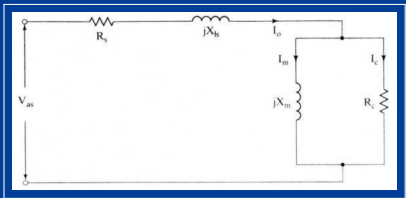


Figure: No-load test circuit

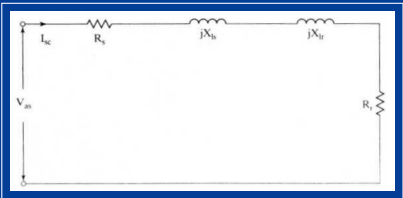


Figure: Blocked rotor test circuit

ACIM Parameter Estimation Formulas

No-Load Test:

$$\cos \phi_0 = \frac{P_i}{V_{\text{as}} I_0}$$

$$I_m = I_0 \sin \phi_0$$

$$I_c = I_0 \cos \phi_0$$

$$L_m = \frac{V_{\text{as}}}{2\pi f_i I_m}$$

$$R_c = \frac{V_{\text{as}}}{I_c}$$

Blocked Rotor Test:

$$\cos \phi_{\text{sc}} = \frac{P_{\text{sc}}}{V_{\text{sc}} I_{\text{sc}}}$$

$$Z_{\text{sc}} = \frac{V_{\text{sc}}}{I_{\text{sc}}}$$

$$R_r = Z_{\text{sc}} \cos \phi_{\text{sc}} - R_s$$

$$X_{\text{eq}} = Z_{\text{sc}} \sin \phi_{\text{sc}}$$

$$X_{\text{eq}} = X_{\text{ls}} + X_{\text{lr}}$$

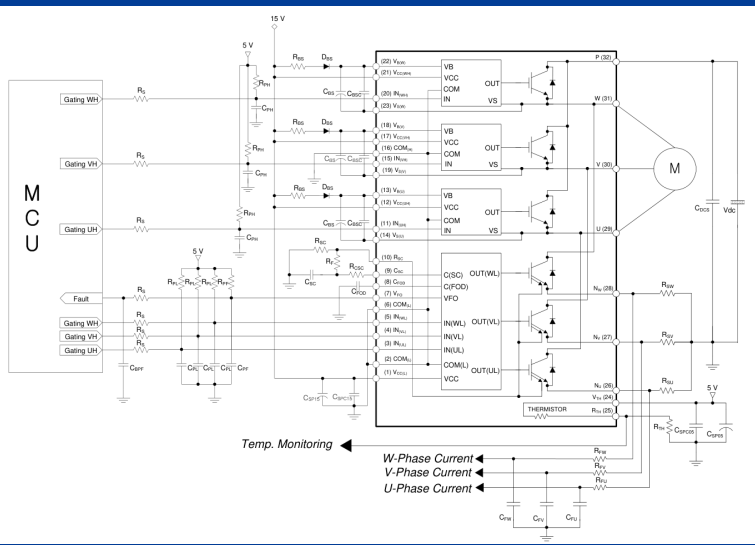
ACIM Parameter Estimation Results

| Sensorless FOC 3PH parameter estimation | | | | |
|---|---------------------------------------|-------------|------------------|---|
| Sno | TESTS to DO | Parameters | 1 | 2 |
| 1 COLD TEST | DC STATOR RESISTANCE(Ohms) | 65 | 60.8 | |
| | Temperature | Rated value | Room temperature | |
| 2 NO LOAD TEST | INPUT ACTIVE POWER , PH(Watts) | 38.33 | 21.67 | |
| | INPUT STATOR VOLTAGE (Line to Line)* | 415.00 | 350.00 | |
| | INPUT STATOR VOLTAGE (Phase) | 239.60 | 202.07 | |
| | INPUT STATOR CURRENT , PH | 0.77 | 0.63 | |
| | POWER FACTOR MEASURED | 0.20 | 0.19 | |
| | PHI (radians) | 1.37 | 1.38 | |
| | Ia(A) | 0.75 | 0.62 | |
| | Ic(A) | 0.15 | 0.12 | |
| | Lm(H) | 1.02 | 1.03 | |
| | Rc(Ohm) | 1562.61 | 1789.26 | |
| 3 LOCKED ROTOR TEST | INPUT ACTIVE POWER , PH | 16.67 | 76.67 | |
| | INPUT STATOR VOLTAGE (Line to Line)** | 100.00 | 219.00 | |
| | INPUT STATOR VOLTAGE (Phase) | 57.74 | 126.44 | |
| | INPUT STATOR CURRENT , PH | 0.47 | 1.00 | |
| | POWER FACTOR MEASURED | 0.57 | 0.66 | |
| | PHI (radians) | 0.97 | 0.85 | |
| | Zsc(Ohm) | 123.72 | 126.44 | |
| | Rr(Ohm) | 5.11 | 18.45 | |
| | Xeq(Ohm) | 181.94 | 94.99 | |
| | Xls(Ohm) | 50.97 | 47.49 | |
| | Xlr(Ohm) | 50.97 | 47.49 | |

| No-Load Test | |
|-----------------------|---------|
| Parameter | Value |
| POWER FACTOR MEASURED | 0.20 |
| PHI (radians) | 1.37 |
| Im (A) | 0.75 |
| Ic (A) | 0.15 |
| Lm (H) | 1.02 |
| Rc (Ohm) | 1562.61 |
| Blocked Test | |
| Parameter | Value |
| POWER FACTOR MEASURED | 0.57 |
| PHI (radians) | 0.97 |
| Zsc (Ohm) | 123.72 |
| Rr (Ohm) | 5.11 |
| Xeq (Ohm) | 101.94 |
| Xls (Ohm) | 50.97 |
| Xlr (Ohm) | 50.97 |

Figure: ACIM Parameter Estimation Results

PCB Design



MCU Interface Circuit

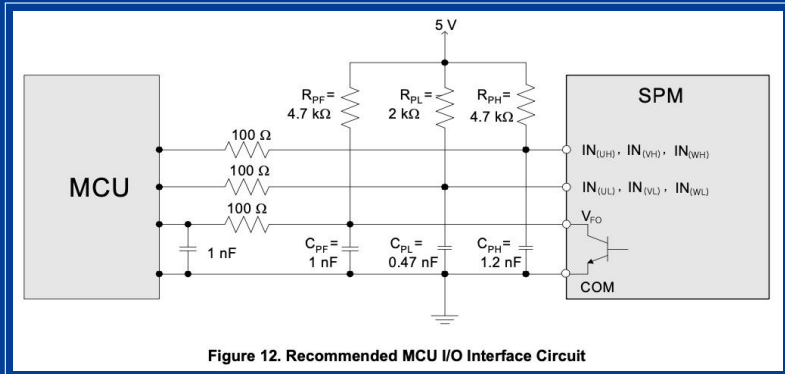


Figure 12. Recommended MCU I/O Interface Circuit

Figure: MCU Interface Circuit

- ▶ Bypass capacitors ground H.F. oscillations, decoupling DC circuit from A.C. Noise.
- ▶ Input pullup removes load strain on MCU.

Short Circuit Protection Circuit

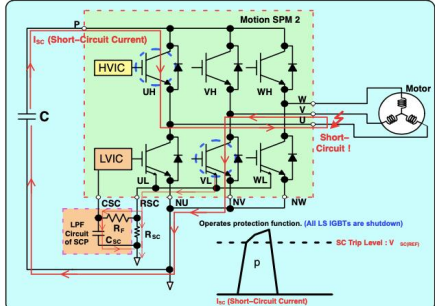


Figure 11. Operation of Short-Circuit Current Protection

Figure: Short Circuit Protection Circuit

- Separate open-emitter pins are provided from low-side IGBTs for current sensing.

Under Voltage Lockout Circuit

| Control Voltage Range [V] | DIP-SPM Function Operations |
|--|---|
| 0 ~ 4 | <u>Control IC does not operate. Under voltage lockout and fault output do not operate.</u> <u>dV/dt noise on the main P-N supply might trigger the IGBTs.</u> |
| 4 ~ 12.5 | <u>Control IC starts to operate. As the under voltage lockout is set, control input signals are blocked and a fault signal F_o is generated.</u> |
| 12.5 ~ 13.5 | Under voltage lockout is reset. IGBTs will be operated in accordance with the control gate input. Driving voltage is below the recommended range so V _{CE(sat)} and the switching loss will be larger than that under normal condition. |
| <u>13.5 ~ 16.5 for V_{CC}</u> <u>13 ~ 18.5 for V_{BS}</u> | <u>Normal operation. This is the recommended operating condition.</u> |
| 16.5 ~ 20 for V _{CC} 18.5 ~ 20 for V _{BS} | IGBTs are still operated. Because driving voltage is above the recommended range, IGBTs' switching is faster. <u>It causes increasing system noise.</u> And peak short circuit current might be too large for proper operation of the short circuit protection. |
| <u>Over 20</u> | <u>Control circuit in the DIP-SPM might be damaged.</u> |

Figure: Under Voltage Lockout Circuit

Bootstrap Circuit

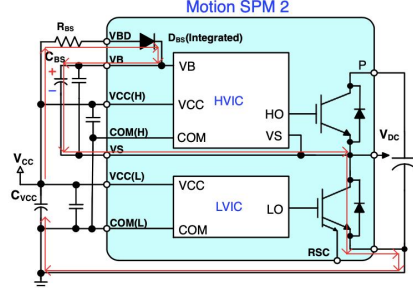


Figure 31. Current Path of Bootstrap Circuit for the Supply Voltage (V_{BS}) of a HVIC when Low-Side IGBT Turns On

Figure: Bootstrap Circuit

- ▶ Charges when low-side switch is on and supplies 15V across high side IGBT gate-emitter

Bootstrap Initial Charging

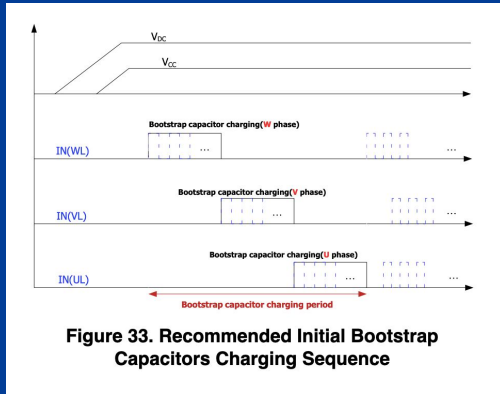


Figure 33. Recommended Initial Bootstrap Capacitors Charging Sequence

Figure: Bootstrap Initial Charging

$$t_{\text{charge}} = C_{BS} \times R_{BS} \times \frac{1}{\Delta} \times \ln \left(\frac{V_{CC} - V_{BS(\min)}}{V_F - V_{LS}} \right) \quad (1)$$

PCB Layout Design

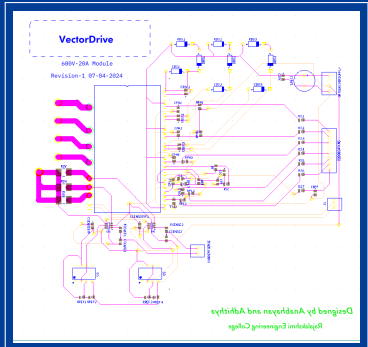


Figure: PCB Layout Design in Ultiboard

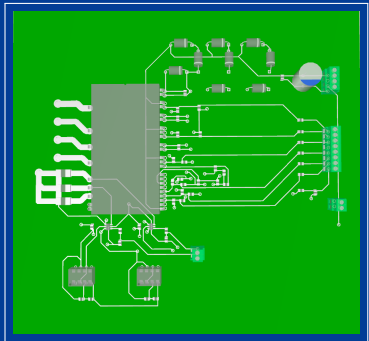


Figure: 3D View of PCB Layout Design in Ultiboard

Rotor Load Angle

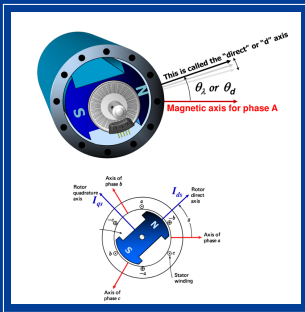


Figure: Rotor Load Angle

Current Sensing Circuit

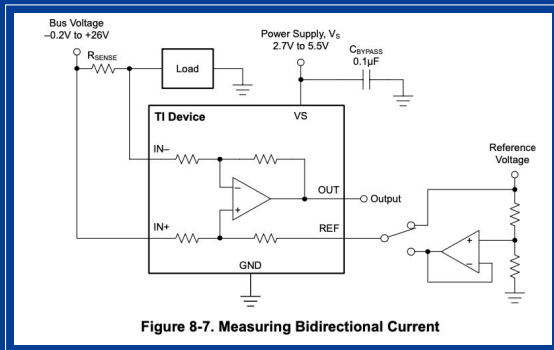


Figure: Current Sensing Circuit

- Differential amplifier is connected across shunt resistor and positive side DC shifted by $\frac{V_{cc}}{2}$ for bi-directional current sensing.

Current Measurement

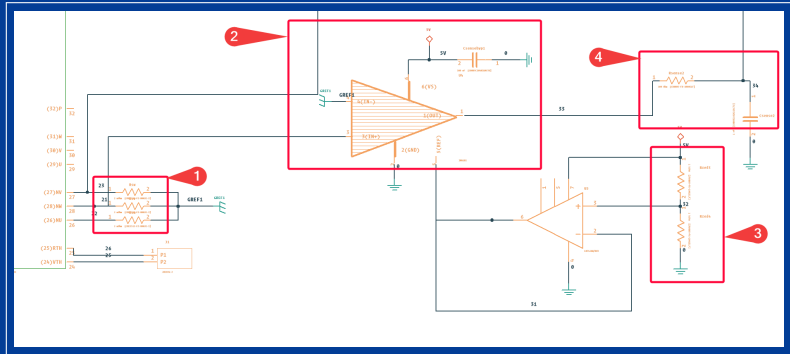


Figure: Current Sensing Circuit in Multisim (one phase shown)

ePWM Module

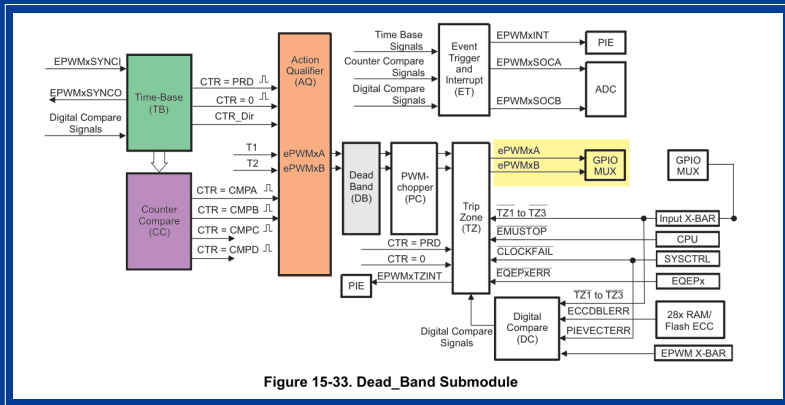


Figure: ePWM Module

ePWM Sub-Module

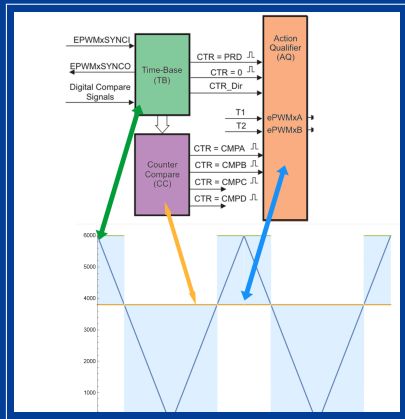


Figure: ePWM Sub-Module

Counter Compare and Timer Period Visualization

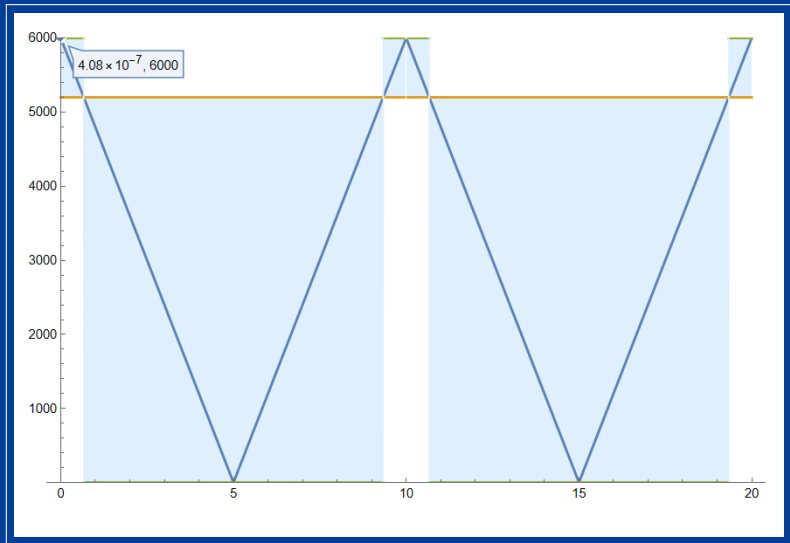


Figure: Counter Compare High

Counter Compare and Timer Period Visualization

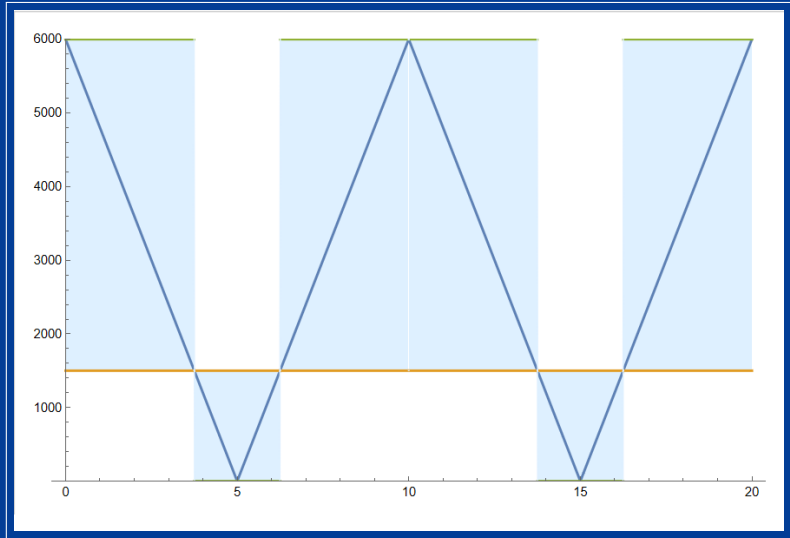


Figure: Counter Compare Low

Counter Compare and Timer Period Visualization

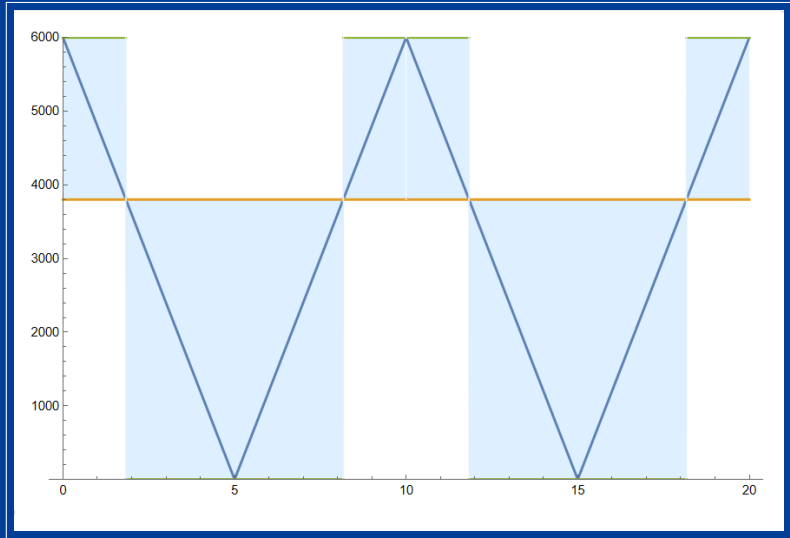


Figure: Counter Compare half

TBPRD Calculation

- ▶ PWM Frequency (F_{PWM}):
15 kHz (recommended by
FSAM20SH60A datasheet)
- ▶ System Clock (SYSCLK):
200 MHz
- ▶ High Speed Clock Divider
(HSPCLKDIV): 1
- ▶ Clock Divider (CLKDIV): 1

$$T_{PWM} = \frac{1}{F_{PWM}}$$

$$T_{TBCLK} = \frac{SYSCLK}{HSPCLKDIV \times CLKDIV}$$

$$TBPRD = \frac{T_{PWM}}{2 \times T_{TBCLK}}$$

$$T_{PWM} = \frac{1}{15 \times 10^3} \text{ seconds}$$

$$T_{TBCLK} = \frac{200 \times 10^6}{1 \times 1} = 200 \times 10^6 \text{ Hz}$$

$$TBPRD = \frac{\frac{1}{15 \times 10^3}}{2 \times 200 \times 10^6} \approx 6667$$

Therefore, the Timer Period (TBPRD) is 6667.

ePWM Configuration

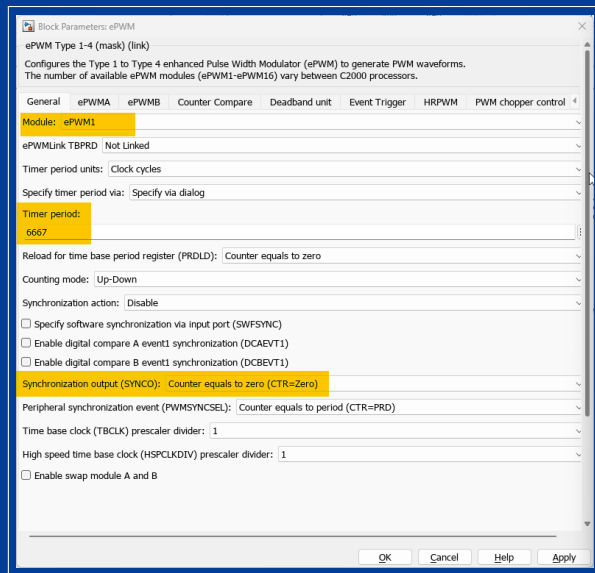


Figure: ePWM configuration in Simulink

SVPWM Switching States

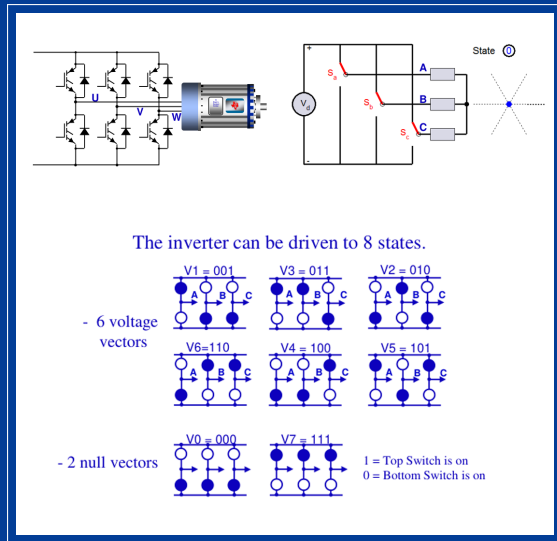


Figure: SVPWM Switching States

SVPWM Gate Pulses

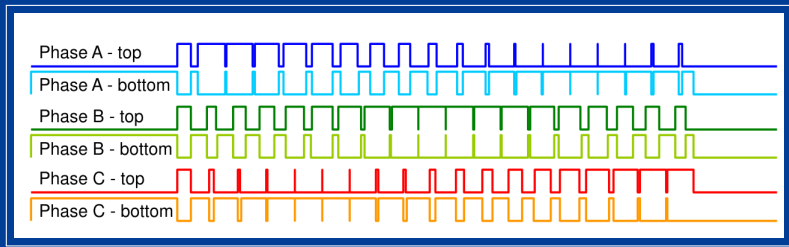


Figure: SVPWM Gate Pulses

Space Vector Pulse Width Modulation (SVPWM)

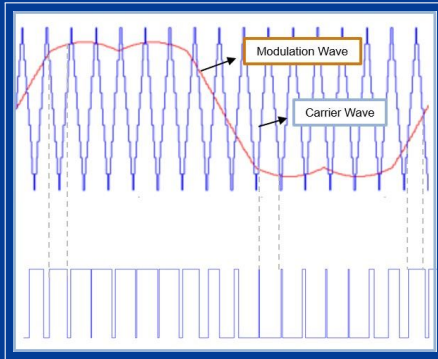


Figure: Gate pulse generation

- ▶ **Increased Efficiency:** SVPWM reduces harmonic distortion.
- ▶ **Higher Voltage Utilization:** SVPWM allows 15% more DC bus voltage.
- ▶ **Reduced Switching Losses**

Open loop: SVPWM

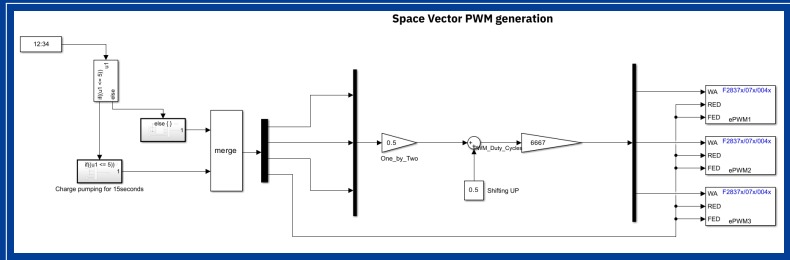


Figure: SVPWM Simulink Model

SVPWM with Low Pass Filter

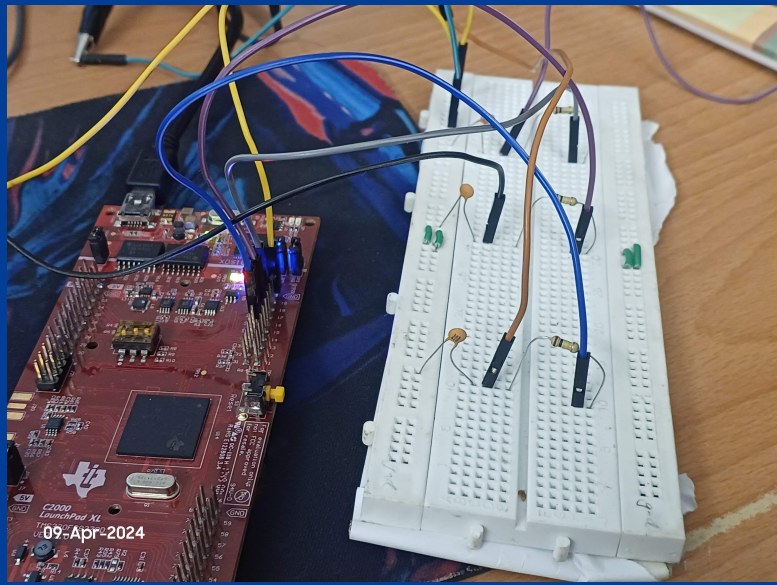


Figure: Hardware setup with RC filter and Launchpad

Output of SVPWM with LPF

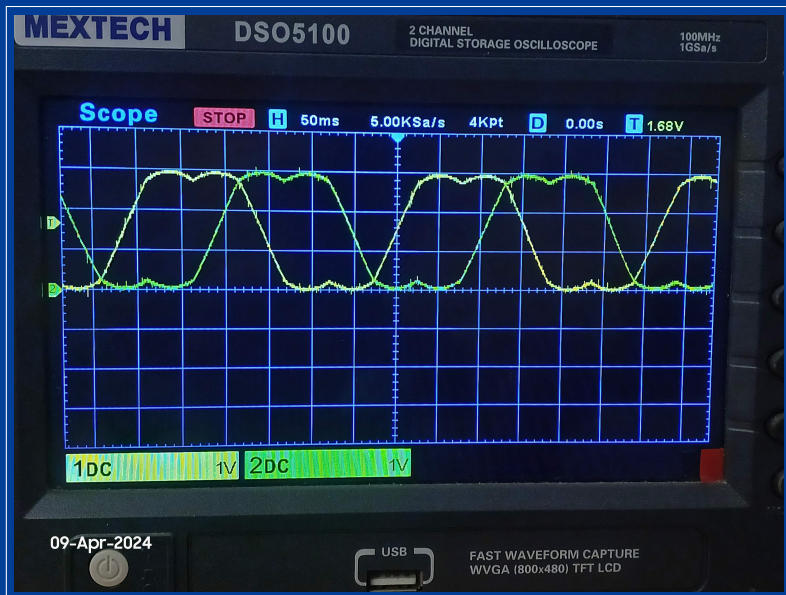


Figure: Output of SVPWM with low pass filter

Dead Band Configuration



Figure: Dead band time

DC Bus Setup

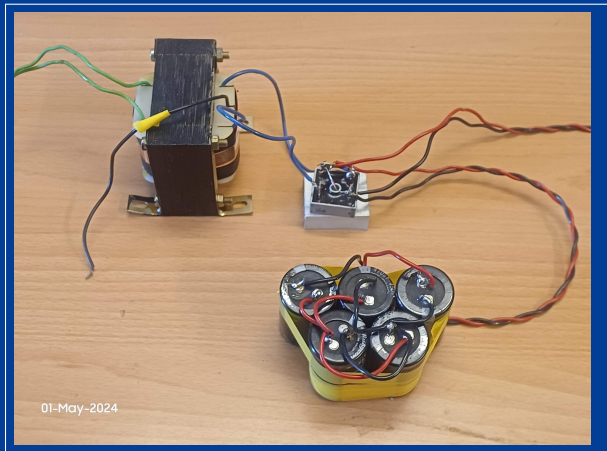


Figure: DC Bus Setup: 230V AC to 48V DC conversion with capacitor banks for stable power delivery

Inverter and Controller

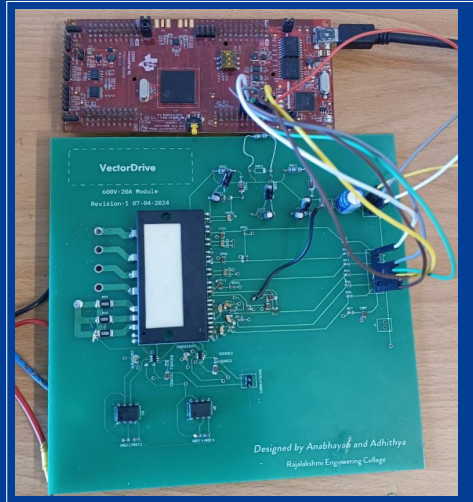


Figure: Inverter (FSAM20SH60A) and Controller (F28379D Launchpad) Setup

Complete Hardware Setup

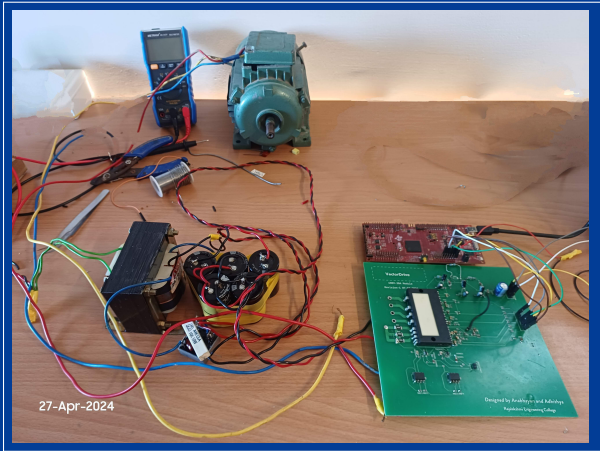


Figure: Experimental Setup for Motor Control System with Induction Motor, DC Bus, Inverter, and Controller

Challenges: False Positives from Fault Alarm

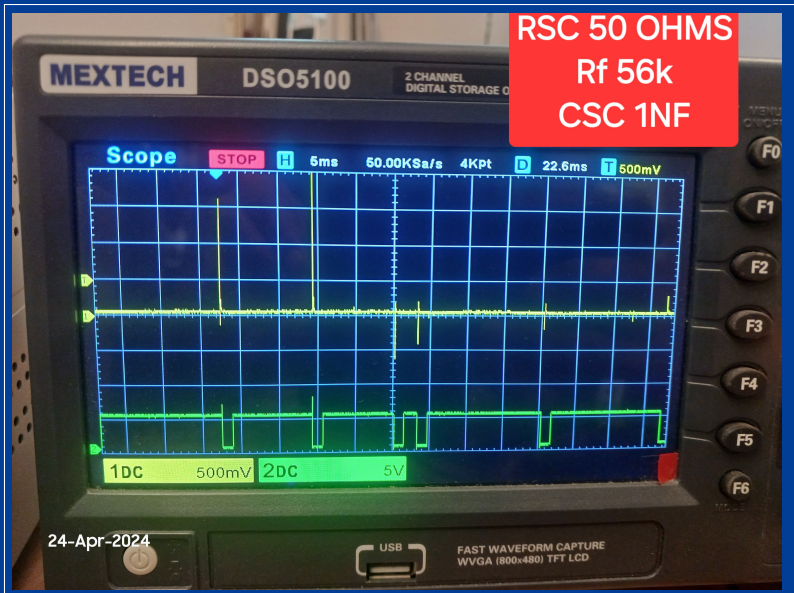


Figure: Vcc Noise and Fault Alarm Signal

Mitigation Strategies

- ▶ **Isolation Attempts:**
 - ▶ Separate control and power stage grounds using separate transformers and rectifiers.
 - ▶ Temporarily shorted RSC and CSC pins to ground to assess external noise influence.
- ▶ **Noise Reduction Techniques:**
 - ▶ Added metal film capacitors across the DC bus to suppress switching transients.
 - ▶ Reduced switching frequency to minimize voltage/current change rate and noise.
- ▶ **Future Considerations:**
 - ▶ Further noise reduction through filtering on control signals and power supply lines.
 - ▶ Improved PCB layout to minimize noise coupling paths and optimize component placement.

Conclusion

- ▶ **Achievements:**
 - ▶ Successful simulation of FOC system demonstrating significant performance improvements.
 - ▶ Design and development of hardware setup including PCB design and component integration.
 - ▶ Identification and analysis of challenges related to noise and false alarms.
- ▶ **Challenges:**
 - ▶ Persistent false positives from the IPM's fault alarm despite implemented mitigation strategies.
 - ▶ Limited hardware validation due to the unresolved fault alarm issue.
- ▶ **Future Work:**
 - ▶ Explore additional noise reduction techniques and PCB layout optimization.
 - ▶ Investigate alternative IPM modules or fault detection mechanisms.
 - ▶ Implement and validate the closed-loop FOC system in hardware upon resolving the challenges.

Literature Review

| Author | Title | Year | Summary |
|--------------------------|--|------|--|
| E.S.Tez | A Simple Understanding Of Field Orientation For Ac Motor Control | 1995 | The article teaches field-orientation for AC motor control, which aligns the stator and rotor fields for fast torque control. It corrects some wrong ideas about motor models and parameters, and shows a new field-orientation design called INVECTOR. |
| Wenzhuo Chen et.al | Simulation of Permanent Magnet Synchronous Motor Field oriented Vector Control System | 2014 | The text describes coordinate conversion's role in managing motor currents, especially excitation and torque. It highlights PI controllers and SVPWM pulses for precise control of PMSM. Simulation results validate the vector control method's accuracy, supporting real-world system design. |
| Dianguo Xu et.al | A Review of Sensorless Control Methods for AC Motor Drives | 2018 | Sensorless control - signal injection methods are simpler and easier to execute than model reference adaptive system and Kalman filter. Requires large amount of data. |
| Rupprecht Gabriel. et al | Implementation of Field Oriented Control for Permanent Magnet Synchronous Motor | 1980 | The article shows how microprocessors can control AC machines better with field orientation, which improves their dynamic performance. It gives the theory of AC motor control by field orientation and some results from a test drive. It explains the induction motor model and talks about the future possibilities in the field. |
| Arun Dominic Dn et.al | Analysis of field-oriented controlled induction motor drives overview of sensorless scheme | 2014 | This article explores use of blanking periods and space vector modulation to enhance low-speed drive performance, providing a thorough technique review. |